Fundamental Research 4 (2024) 1063–1071

Contents lists available at ScienceDirect

Fundamental Research

journal homepage: http://www.keaipublishing.com/en/journals/fundamental-research/

Article

Can software-defined vehicles never roll over: A perspective of active structural transformation

Bowei Zhang [a], Jin Huang [a,*], Jianping Wang [b], Yanzhao Su [a], Jiaxing Li [a], Xiangyu Wang [a], Ye-Hwa Chen [c], Yuhai Wang [d], Zhihua Zhong [a]

[a] School of Vehicle and Mobility, Tsinghua University, Beijing 100084, China
[b] Department of Computer Science, City University of Hong Kong, CYC-6223 Hong Kong, China
[c] The George W. Woodruff School of Mechanical Engineering, Georgia Institute of Technology, Atlanta, GA 30332, USA
[d] FAW Jiefang Automobile Co., Ltd, China

ARTICLE INFO

Article history:
Received 7 January 2023
Received in revised form 2 December 2023
Accepted 4 December 2023
Available online 31 July 2024

Keywords:
Software-defined vehicles
Active structural transformation
Vehicle handling stability
Vehicle ride comfort
Multi-objective optimization

ABSTRACT

The revolution of physical structure is highly significant for future software defined vehicles (SDV). Active structural transformation is a promising feature of the next generation of vehicle physical structure. It can enhance the dynamic performance of vehicles, thus providing safer and more comfortable ride experiences, such as the ability to avoid rollover in critical situations. Based on the active structural transformation technology, this study proposes a novel approach to improve the dynamic performance of a vehicle. The first analytical motion model of a vehicle with active structural transformation capability is established. Then, a multi-objective optimization problem with the adjustable parameters as design variables is abstracted and solved with an innovative scenario specific optimization method. Simulation results under different driving scenarios revealed that the active transformable vehicle applying the proposed method could significantly improve the handling stability without sacrificing the ride comfort, compared with a conventional vehicle with a fixed structure. The proposed method pipeline is defined by the software and supported by the hardware. It fully embodies the characteristics of SDV, and inspires the improvement of multiple types of vehicle performance based on the concept of "being defined by software" and the revolution of the physical structure.

1. Introduction

The global automobile industry is strategically moving toward intelligent vehicles. The evolution of intelligent vehicles will be reflected in the improvement of the user experience, which is enabled by technological advancements. Software drives innovation in automotive technologies. Therefore, the concept of software-defined vehicles (SDVs) is becoming an important trend in the vehicle industry [1–3]. The core characteristics of the SDV can be summarized as the realization of various intelligent algorithms and functions supported by both the new software and the new physical architecture.

Recently, close attention has been paid to the characteristics of the SDV, focusing mainly on vehicular networks and vehicle software architectures. Early in-vehicle software and networks, such as Google Android [3] and GENIVI [4], were generally used as infotainment facilities. The rapid advancement of information technology has led to the integration of core driving with software systems. The AUTOSAR standard [5,6] provides software architecture support for a wide range of vehicle-side task requirements, including aided driving and self-driving [7]. Software under this standard must be supported by novel electrical and electronic (EE) architectures including distributed EE systems and in-vehicle networks of novel types (LIN [8], FlexRay [9], etc.). In addition to the functionality of a single vehicle, the "vehicle to everything" concept is also within the scope of the SDV. Representative studies mainly focused on the over-the-air software updating technology [10,11], software defined vehicular networks [12–14] and the vehicular cloud [15,16].

From a software perspective, innovative research has been conducted to popularize the concept of the SDV. However, the hardware to accompany the developing software also needs a revolutionary upgrade, and the absence of the corresponding features of the hardware remains problematic. A key focus of the SDV is to make a vehicle sufficiently scalable and customizable, which the embedded hardware should be able to accommodate. The active structural transformation capability should be an important characteristic of the SDV hardware to customize future vehicles. This capability refers to the autonomous adjustment of the inherent structural parameters of a vehicle based on the user's needs. Various attributes of a vehicle are strongly related to its structural parameters.

* Corresponding author.
E-mail address: huangjin@tsinghua.edu.cn (J. Huang).

https://doi.org/10.1016/j.fmre.2023.12.024

The active transformation technology can adjust vehicle performance on demand and significantly improve user experience.

Breakthroughs on active structural transformation have been made in research on the deformation of mechanical systems such as robots. Some deformation mechanisms have been applied to enhance versatility of the robots [17–20]. Studies on the deformation of vehicles can be divided into two categories: structural parameter adjustment and physical topology transformation. Vehicles adopting the former maintain their general physical topology while simply adjusting some key parameters, mostly the wheelbase, the wheel track, or the stiffness and damping of the suspension systems. In [21], a wheelbase adjustment mechanism and the mechanical structure of a three-axle all-terrain vehicle were designed thus enhancing the adaptability to different terrains. In [22], an innovative vehicle yaw moment control system was described, in which the longitudinal positions of the wheels were individually controlled. A model- free successor to this control method based on the active transformation of the structure was applied to a four-wheel independent steering unmanned ground vehicle [23]. Several studies on the design and control of active suspension systems also contributed significantly to developing the adjustment mechanisms of structural parameters [24–27]. Vehicles adopting the latter can significantly change their physical topology according to different requirements. In [28], the prototype and control strategy of a foldable micro electric vehicle were designed for flexible driving in urban scenarios. In [29], the deformation of the conceptual prototype of a personal mobility vehicle was realized through the special-designed structure. Several original equipment manufacturers have introduced electric concept cars with deformation capabilities and their principle prototypes, such as iEV Motor's iEV X and iEV Z and Audi's Skysphere. However, a comprehensive mathematical description of the active transformation is still lacking, thus hindering the correlation between the active transformation and multiple types of vehicle performance.

Here, based on the technical progress introduced above, the potential for further improving the dynamic performance of vehicles through the active structural transformation technology was explored. In some critical driving scenarios, vehicles can lose stability and even suffer from accidents like tail- flip, rollover (Fig. 1), and jolts. Meanwhile, a trade-off always exists between some types of dynamic features. For instance, limiting the roll angle of the vehicle body by increasing the suspension stiffness may lead to extra vertical vibration. However, with the support of active structural transformation, fine-tuning structural parameters enables the vehicle to meet dynamic performance requirements in different conditions. It can also prevent the loss of stability under extreme conditions to avoid fatal accidents. By establishing the longitudinal and lateral motions and vertical vibration model of an active transformable vehicle and describing the analytical relationship between the dynamic performance and adjustable structural parameters, a multi-objective optimization (MOO) problem is formulated and solved. To the best of the authors' knowledge, this work is the first to emphasize the structural aspect in the development of the SDV, and specify it through transferring the real-time dynamic performance enhancement of vehicles to an MOO problem aided by the active structural transformation technology. The main contributions of this study are threefold. First, the overall motion model of the active transformable vehicle is established to reveal the analytical relationship between the dynamic performance and the adjustable structural parameters. To this end, part of the mathematical model of the hardware architecture of the active transformable SDV is proposed. Second, enhancing the dynamic performance of the vehicle is converted into an MOO problem. Its solution is defined by the software and supported by the hardware. Third, the nondominated sorting genetic algorithm II (NSGA- II) method is adopted to solve the MOO problem, and a scenario-adaptive Pareto-rank rule is utilized to find the trade-off point on the Pareto front as the final decision for adjustable parameters. Simulation results revealed that, compared with conventional vehicles with fixed structural parameters, the proposed method could help vehicles with the active transformation ability achieve better handling stability in different driving scenarios, including extreme conditions, without sacrificing ride comfort. This study brings a novel perspective to enhancing the safety and ride comfort of future vehicles and future studies on SDV technologies.

Fig. 1. Vehicle tail-flip and rollover caused by poor dynamic performance leading to severe crash.

2. Motion model of active transformable vehicle

The dynamic model of an active transformable vehicle is established to derive the maps between the adjustable structural parameters and evaluation metrics of dynamic performance. The adjustable parameters are illustrated in Fig. 2. It is assumed that the basic configuration of the vehicle is the same as that of a common two-axle car. The tuple of adjustable parameters is $\theta = [a \quad L \quad k_s \quad C_s \quad h \quad B]^T$, where a represents the distance between the front axle and the center of gravity (C.G.). L represents the wheelbase. k_s and C_s represent the linear stiffness and damping of the suspension system, respectively. h represents the height of the C.G., and B represents the wheel track. As mentioned in Section 1, dynamic performance enhancement attempts to improve the driving safety of the vehicle by enhancing the handling stability without sacrificing the ride comfort of passengers.

2.1. Motion model for handling assessment

When modeling the motion of a vehicle to assess handling stability on the planar road, it is common to employ a simplified two-degree-of-freedom bi- cycle model. According to Newton's laws of motion, the equations of motion of the active transformable vehicle can be expressed as

$$m\dot{v}_x + \mu_G mg + \mu_D \dot{v}_x^2 = F_d, \tag{1}$$

$$\mathrm{m}v_x\left(\frac{v_y}{v_x} + \omega_r\right) = F_f + F_r, \tag{2}$$

$$\mathrm{I}_z\dot{\omega}_r = F_f\left(a_0 + \Delta a\right) - F_r\left(L_0 + \Delta L - a_0 - \Delta a\right). \tag{3}$$

The longitudinal motion is described by (1), where m denotes the total mass, v_x denotes the longitudinal velocity, μ_G and μ_D are the coefficients of friction and air drag, respectively, and F_d represents the driving

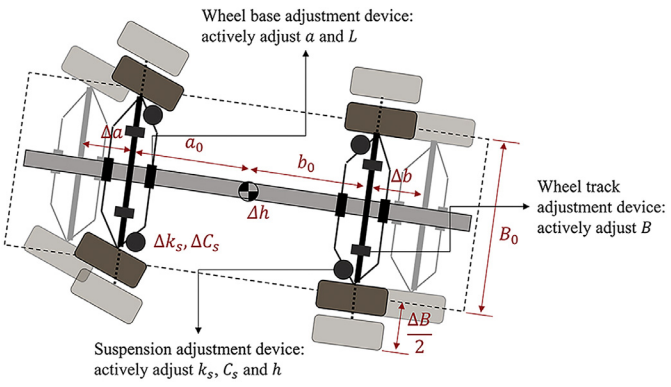

Fig. 2. Concept of active structural transformation realized by adjusting the key parameters of the vehicle.

force. The lateral motion is described by (2) and (3), where $\beta = \frac{v_y}{v_{v_x}}$ is the ratio of the lateral and longitudinal velocities, ω_r is the yaw rate, F_f and F_r represent the front and rear lateral forces of the tire, respectively, and a and L represent the distance from the C.G. to the front axle and the wheelbase, respectively. Symbols $()_0$ and $\Delta()$ refer to the initial value and change amount for all adjustable parameters, respectively. The yaw moment of inertia is approximated as

$$\mathrm{I_z} = I_{z,0}\left(\frac{L_0 + \Delta L}{L_0}\right) \tag{4}$$

for simplicity. This plain model can describe the vehicle dynamics in most cases. However, it neglects the influence of the suspension system on the lateral motion of the vehicle. This influence, mainly caused by the rolling– steering coupled effect, is critical when considering the context of active structural transformation.

To establish a more accurate and comprehensive model for deriving optimal parameters, the rolling of the vehicle body cannot be neglected when describing the transient response. Let ϕ be the roll angle and the vehicle model is symmetric about the x–axis. The coupled lateral motion model can then be rewritten as

$$\mathrm{mv_x}\left(\frac{\dot{v}_y}{v_x} + \omega_r\right) = m_s h_s \ddot{\phi} + F_f + F_r, \tag{5}$$

$$\mathrm{I_z}\dot{\omega}_r = F_f\left(a_0 + \Delta a\right) - F_r\left(L_0 + \Delta L - a_0 - \Delta a\right), \tag{6}$$

$$\mathrm{I_x}\ddot{\phi} = m_s h_s v_x\left(\frac{\dot{v}_y}{v_x} + \omega_r - \frac{\ddot{\phi}}{v_x}h_s\right) + \mathrm{m_s}g h_s \phi - M_\phi, \tag{7}$$

according to the D'Alembert's principle and the angular momentum theorem. Here m_s is the sprung mass and h_s is the distance between the C.G. and the rolling axis. In (5), $m_s h_s \ddot{\phi}$ represents the inertial force caused by rolling motion. In (7), I_x is the rolling moment of inertia, while M_ϕ refers to the rolling resistance caused by the suspension system. Assuming that the height of the C.G. and the roll centers of the suspension system h_f and h_r rise and fall consistently, h_s can be expressed as

$$\mathrm{h_s} = \left(h_0 + \Delta h\right) - \frac{\left(h_{f0} + \Delta h\right)\left(L_0 + \Delta L - a_0 - \Delta a\right)}{L_0 + \Delta L} - \frac{\left(h_{r0} + \Delta h\right)\left(a_0 + \Delta a\right)}{L_0 + \Delta L}. \tag{8}$$

The expression of M_ϕ is

$$\mathrm{M}_\phi = \lambda_k\left(k_{s,0} + \Delta k_s\right)\phi + \lambda_C\left(C_{s,0} + \Delta C_s\right)\dot{\phi}, \tag{9}$$

where λ_k and λ_C are the transfer factors from linear parameters to their angular counterparts. By analyzing the total torque of the vehicle body around the rolling axis using the D'Alembert's principle, we can obtain a description of the critical state of rollover. Let

$$T \coloneqq -\frac{1}{B}\left(m_s g\left(\frac{B}{2} - \left(h - h_r\right)\sin\phi\right) - m_s a_y\left(h_r + \left(h - h_r\right)\cos\phi\right) - \tilde{I}_x\ddot{\phi}\right), \tag{10}$$

where $\tilde{I}_x$ refers to the roll moment of inertia about the rolling axis, and can be approximated as

$$\tilde{I}_x \approx I_x - m_s\left(h - h_r\right)^2 + m_s(h + B)^2 \tag{11}$$

for simplicity according to the parallel-axis theorem of the rigid body. Therefore, T is the normal force exerted on the inside wheel by the ground. Rollover accidents can occur if $T \le 0$.

Remark 1. It is assumed that the parameters of the front and rear suspension systems, including $\mathrm{k_s}$, $\mathrm{C_s}$, λ_k and λ_C are equal in the dynamic model to simplify the analysis. In practice, they can be adjusted synchronously and simultaneously by the fully-active suspension system.

Remark 2. Because changing the wheelbase B alone has little effect on $\mathrm{I_x}$, it is assumed to be a constant in the model.

Without loss of generality, the pure-lateral-slip magic formula tire model proposed by Pacejka [30] is employed to describe the lateral force of each wheel, which is a function of the slide-slip angle α and the normal load force F_z on the tire in the absence of the camber angle, i.e.,

$$\mathrm{F_i} = F_i\left(F_{zi}, \alpha_i\right), i = fl, rl, fr, rr. \tag{12}$$

Then we have

$$\mathrm{F}_f = F_{fl} + F_{fr}, \mathrm{F}_r = F_{rl} + F_{rr}. \tag{13}$$

If μ is the road adhesion coefficient, the expression of F_i is

$$\mathrm{F_i} = \mu D \sin\left(C\arctan\left(G\alpha_i - E\left(G\alpha_i - \arctan\left(G\alpha_i\right)\right)\right)\right). \tag{14}$$

To determine the coefficients in (14), Pacejka introduced a series of constant scalars $\{\gamma_i\}$, $i = 0, 1, 2, 3, 4, 5, 6$, and defined the coefficients as

$$\mathrm{C} = \gamma_0, D = \gamma_1 F_{zi}^2 + \gamma_2 F_{zi},$$

$$E = \gamma_5 F_{zi} + \gamma_6, G = \frac{\gamma_3 \sin\left(2\arctan\frac{F_{zi}}{\gamma_4}\right)}{CD}. \tag{15}$$

The value of $\{\gamma\mathrm{i}\}$ was given in [31]. Considering the roll-interference effect, the front and rear side–slip angles can be expressed as

$$\alpha_{fl} = \alpha_{fr} = \beta + \frac{\left(a_0 + \Delta a\right)\omega_r}{v_x} - \delta + \xi_\mathrm{f}\phi,$$

$$\alpha_{fr} = \alpha_{rr} = \beta - \frac{\left(L_0 + \Delta L - a_0 - \Delta a\right)\omega_r}{v_x} + \xi_r\phi, \tag{16}$$

with simple geometrical analysis, where $\xi_{f,r} = \frac{\partial\alpha_{f,r}}{\partial\phi}$ is the rolling-interference coefficient of steering. It is assumed that the longitudinal speed is constant and the normal load forces on each axle are only influenced by the position of the C.G. According to the moment equation in the non-inertial frame, the normal forces can be expressed as

$$\mathrm{F}_{z_{fl,fr}} = \frac{L_0 + \Delta L - a_0 - \Delta a}{L_0 + \Delta L}\left(\frac{mg}{2} \pm \frac{h_0 + \Delta h}{B}F_n\right),$$

$$\mathrm{F}_{z_{rl,rr}} = \frac{a_0 + \Delta a}{L_0 + \Delta L}\left(\frac{mg}{2} \pm \frac{h_0 + \Delta h}{B}F_n\right), \tag{17}$$

where

$$\mathrm{F_n} = m_s\left(\dot{\beta} + \omega_r - \frac{\ddot{\phi}}{u}h_s\right) + \mathrm{m_{\bar{s}}}\left(\dot{\beta} + \omega_r\right), \tag{18}$$

with m_s as the unsprung mass. Adopting numerical methods, we can solve the differential equation set that describes the rolling–steering coupled transient response of a vehicle, given the steer angle input.

2.2. Motion model for ride comfort assessment

A half-vehicle vertical motion model with a pair of road excitation inputs and its corresponding single-wheel-input model are established to analyze the vertical vibration for ride comfort assessment. The single-wheel-input equivalent method loosens the coupling of the vibration of the front and rear axles, thus simplifying the analysis without losing much precision.

The sprung mass of a half-vehicle model can be decomposed into three parts: the mass$_y$ above the front axle (m_{sf}), above the rear axle (m_{sr}) and on the C.G. (m_{sc}). If $m_{sc} = 0$, then the vertical vibrations of m_{sf} and m_{sr} are independent. With ρ_y as the pitch radius, we obtain

$$\mathrm{m_s}\rho_y^2 = m_{sf}\left(a_0 + \Delta a\right)^2 + m_{sr}\left(L_0 + \Delta L - a_0 - \Delta a\right)^2, \tag{19}$$

$$\mathrm{m_{sc}} = m_s\left(1 - \frac{\rho_y^2}{\left(a_0 + \Delta a\right)\left(L_0 + \Delta L - a_0 - \Delta a\right)}\right). \tag{20}$$

Let $\psi \coloneqq \frac{\rho_y^2}{ab}$ denote the sprung mass distribution coefficient. Assuming that $\psi = 1$, the vertical motion of an arbitrary point P on the vehicle body can be expressed as

$$z_{\mathrm{sP}}(t) = z_{sf}(t) + \frac{l}{L_0 + \Delta L}\left(z_{sf}(t) - z_{sr}(t)\right), \tag{21}$$

where l is the perpendicular distance between P and the front axle, and $z_{sf}(t)$ and $z_{sr}(t)$ are the vertical displacement of m_{sf} and m_{sr}, respectively, which satisfy

$$z_{sr}(t) = z_{sf}\left(t - \frac{L_0 + \Delta L}{v_x}\right), \tag{22}$$

and z_{sf} can be calculated by solving

$$\begin{aligned} &m_{sf}\ddot{z}_{sf}(t)+\left(C_{s0}+\Delta C_s\right)\left(\dot{z}_{sf}(t)-\dot{z}_{\bar{s}f}(t)\right)+\left(k_{s0}+\Delta k_s\right)\left(z_{sf}(t)-z_{\bar{s}f}(t)\right)=0,\\ &m_{\bar{s}f}\ddot{z}_{\bar{s}f}(t)+\left(C_{s0}+\Delta C_s\right)\left(\dot{z}_{\bar{s}f}(t)-\dot{z}_{sf}(t)\right)\\ &+\left(k_{s0}+\Delta k_s\right)\left(z_{\bar{s}f}(t)-z_{sf}(t)\right)+k_t\left(z_{sf}(t)-q(t)\right)=0, \end{aligned} \tag{23}$$

where $z_{s\text{-}f}$ is the vertical displacement of the front unsprung mass and k_t is the linear stiffness of the tires.

The above model describes the vertical motion of the body of the active structural transformable vehicle under road excitation in the time domain.

3. Optimization problem formulation

3.1. Problem statement

With the aforementioned motion model, the dynamic performance enhancement can be converted to an MOO problem aided by the active structural transformation technology. A scenario in which the vehicle makes a sudden J-turn on the rough road was considered, as illustrated in Fig. 3. This type of driving behavior often occurs during emergencies, and has rather high requirements for vehicle handling stability and ride comfort.

Based on the motion model, the following optimization objectives were selected to assess the dynamic performance under the driving scenario:

- κ is the overshoot of the yaw rate ωr given a step input of the steering angle. It reflects the precision of the yaw rate reaction.
- ϕm is the maximal roll angle of the vehicle body given a step input of the steering angle. It reflects the stability of the vehicle body.
- aw is the average acceleration level of vertical vibration of the sprung mass in the entire driving stage (tested on a fixed point on the vehicle body). It reflects the ride experience of the passengers.

The design parameter $\Delta\theta$ refers to the change in the adjustable parameters relative to a predefined base θ_0. The MOO problem for the dynamic performance enhancement of an active transformable vehicle can now be pro- posed as follows:

Problem 1. *(Dynamic Performance Optimization):*

$$\min_{\Delta\theta}\left\{\kappa(\Delta\theta), \phi_m(\Delta\theta), a_w(\Delta\theta)\right\},$$

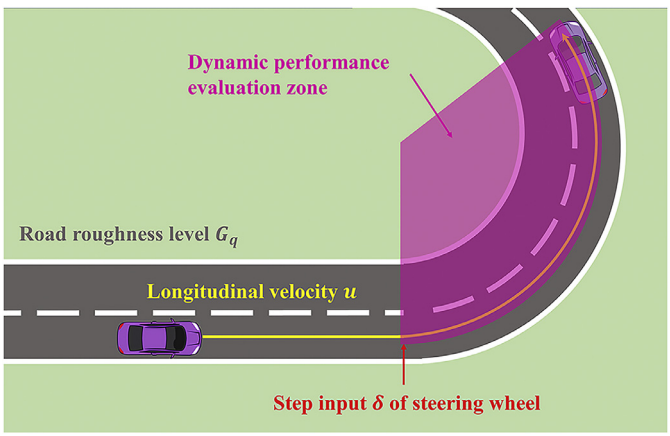

Fig. 3. Driving scenario of dynamic performance evaluation.

subject to

$$\Delta\theta \in \mathbb{C}_1 \cap \mathbb{C}_2$$

where

$$\begin{aligned} \mathbb{C}_1 = &\left[\underline{\Delta a}, \overline{\Delta a}\right] \times \left[\underline{\Delta L}, \overline{\Delta L}\right] \times \left[\underline{\Delta k_s}, \overline{\Delta k_s}\right] \times \left[\underline{\Delta C_s}, \overline{\Delta C_s}\right] \times \left[\underline{\Delta h}, \overline{\Delta h}\right]\\ &\times\left[\underline{\Delta B}, \overline{\Delta B}\right], \end{aligned}$$

$$\mathbb{C}_2 = \{\Delta\theta | 1-\epsilon < \psi(\Delta\theta) < 1+\epsilon\},$$

with ϵ as a small constant.

Remark 3. The constraints of the design parameters are specified with two sets: C_1 and C_2. C_1 refers to the lower and upper boundary of the change amount of each adjustable parameter. Various factors, including the mechanical limitation and user requirements, can restrict the $\Delta\theta$ range. This study neglects the boundary design. C_2 refers to the assumption in the modeling of vertical vibration. When ε is small, $\psi(\Delta\theta) \approx 1$. Then (21) and (22) hold.

3.2. Evaluation metrics analysis

With the motion model of an active transformable vehicle established, we can derive the numerical or analytical expression of the evaluation metrics, i.e., the optimization objectives of the MOO problem.

By solving (5)-(7), we can obtain the rolling–steering coupled transient response of an active transformable vehicle. When $\omega_r = \omega_r(\Delta\theta, t)$ and $\phi = \phi(\Delta\theta, t)$ are the solutions of the yaw rate and roll angle, respectively, and $\omega_{r\infty}(\Delta\theta) = \lim \omega_r(\Delta\theta, t)$ is the steady value of the yaw rate, the overshoot $\kappa(\Delta\theta)$ can be represented as

$$\kappa(\Delta\theta) = \frac{\max\left(\omega_r(t,\Delta\theta)\right) - \omega_{r_\infty}}{\omega_{r_\infty}}, \tag{24}$$

and the maximum of the roll angle as

$$\phi_m(\Delta\theta, t) = \max \phi(\Delta\theta, t). \tag{25}$$

By transferring (23) into the frequency domain and conducting mathematical processing, the transfer function $|\frac{\tilde{z}_{2f}(f)}{q(f)}|$ can be derived as

$$\left|\frac{\tilde{z}_{2f}(f)}{q(f)}\right| = \frac{1}{\mathrm{Y}}\left(\frac{k_t}{k_{s0}+\Delta k_s}\right)^2\left(1+\frac{4\pi^2 f^2\left(C_{s0}+\Delta C_s\right)^2}{\left(k_{s0}+\Delta k_s\right)^2}\frac{m_{\bar{s}f}m_{sf}}{\mu_m}\right), \tag{26}$$

$$\begin{aligned} \mathrm{Y} = &\left[\left(1-\frac{4\pi^2 f^2 m_{sf}}{k_{s0}+\Delta k_s}\right)\left(1+\frac{k_t-4\pi^2 f^2 m_{\bar{s}f}}{k_{s0}+\Delta k_s}\right)-1\right]^2\\ &+\frac{m_{\bar{s}f}^2\left(C_{s0}+\Delta C_s\right)^2}{m_{sf}\left(k_{s0}+\Delta k_s\right)}\left[\frac{k_t}{k_s}-\frac{4\pi^2 f^2 m_{sf}}{k_{s0}+\Delta k_s}\left(\frac{m_{\bar{s}f}}{m_{sf}}+1\right)^2\right]. \end{aligned} \tag{27}$$

Then the weighted level of vertical acceleration a_w can be calculated by

$$\mathrm{a_w} = \left[\int_{\underline{f}}^{\bar{f}} w^2(f) G_a(f) df\right]^{\frac{1}{2}}, \tag{28}$$

where $w(f)$ is the weight function of the frequency, and $\underline{f}$ and $\bar{f}$ is the lower and upper bound of f, as reported in [32]. From Eqs. 24,25 and (28) we can find that, in addition to $\Delta\theta$, the three evaluation metrics are influenced by external factors, including the longitudinal velocity v_x, steering angle given by the driver δ, and power spectrum of road excitation $G_q(n_0)$, which are considered as "environmental conditions".

In this section, the relationship between the evaluation metrics of the dynamic performance and the adjustable structural parameters is established utilizing the corresponding vehicle models. The map

$$\Delta\theta \rightarrow \left[\kappa(\Delta\theta), \phi(\Delta\theta), a_w(\Delta\theta)\right]^T \tag{29}$$

is formed and the image serves as the objectives of the MOO problem. Consequently, part of the mathematical model of the active transformable SDV is proposed from the perspective of vehicle dynamics.

4. Dynamic performance enhancement via multi-objective optimization

Although conflicts exist between handling and ride comfort, the objective of MOO is to seek the optima of all the evaluation metrics simultaneously with the help of the active transformation technology. From the game theory perspective, the MOO problem defined in Section 3 attempts to determine a decision tuple (i.e., the optimal parameters) to minimize each player's cost (i.e., the evaluation metrics). According to economist Pareto, a decision N-tuple is considered optimal if and only if one of two situations occurs: adopting another joint decision either 1) results in no change in any of the costs or 2) results in a cost increase to at least one player. Such Pareto optimal decisions are considered solutions to the MOO problem.

Many strategies have been recently explored to determine the Pareto optima for MOO problems. One strategy involves utilizing the analytical method based on the definition and corresponding lemma [33,34]. Analytical methods can obtain the exact Pareto optima in theory, however, they require and explicit relationship between the decision tuple and costs $J_i = J_i(d)$, which is difficult to derive in most cases, including this study. Another strategy involves the utilization of numerical or soft computing methods, among which the family of genetic algorithms (GAs) [35,36] has gained popularity owing to its effectiveness in addressing nonlinear problems and reducing the possibility of converging to a local minimum. NSGA-II [37], a widely-used meta-heuristic optimization method, is adopted herein to optimize the adjustable structural parameters of the vehicle. The NSGA-II procedure begins with a randomly selected population sorted according to the non-domination principle. The first generation is created using binary selection, crossover, and mutation, as in the usual GA methods. After the first generation, the population is compared with the previously obtained non-dominated solutions to select elites. To develop a novel population, binary selection based on non-domination and crowding distance is utilized, followed by crossover and mutation. This type of crowded distance sorting is applied using crowding distance values. These values measure the objective space around the solution that is not occupied by any other solution in that population.

The decision tuples on the Pareto fronts are all optimal according to the cooperative game theory because none of those tuples can dominate the others in terms of the optimization objects. However, with different optimal structural parameters, active transformable vehicles exhibit different dynamic characteristics. Meanwhile, the requirements for dynamic performance often vary with environmental conditions. Consequently, for a certain scenario, decision tuples on the Pareto fronts are all *optimal*, but not all are *suitable*. Selecting a trade-off optimal point on the Pareto fronts for a proper compromise among all objectives is necessary. A Pareto rank method is designed and applied to determine the trade-off point. The procedure is as follows:

1) The optimization objectives are normalized utilizing the min-max normalization method. The the symbol $\tilde{(\cdot)}$ is defined as the min-max normalization operator. Then we have

$$\tilde{p} = \frac{p - \min p}{\max p - \min p}, p = \kappa, \phi, a_w. \tag{30}$$

2) The weights of summation $[\alpha(\mathcal{E}) \quad \beta(\mathcal{E}) \quad \gamma(\mathcal{E})]^T$ are determined according to the environmental factors $\mathcal{E} = [v_x \quad \delta \quad G_q(n_0)]^T$ and the weights are normalized. In the dynamic model established, all the optimization objectives increase with the increase in v_x, and with increasing δ, ϕ_m increases while κ remains nearly unchanged. The vertical acceleration level a_w increases with increasing $G_q(n_0)$, whereas κ and ϕ_m are nearly unaffected by $G_q(n_0)$. The following rules are proposed to determine the summation weights:

$$\alpha(\mathcal{E}) = C_0 + \tilde{v}_x^{\sigma_\alpha(v_x)},$$

$$\beta(\mathcal{E}) = C_0 + \tilde{v}_x^{\sigma_\beta(v_x)} \tilde{\delta}^{\sigma_\beta(\delta)},$$

$$\gamma(\mathcal{E}) = C_0 + \tilde{v}_x^{\sigma_\gamma(v_x)} \tilde{G}_q(n_0)^{\sigma_\gamma(G_q(n_0))},$$

$$\begin{bmatrix} \hat{\alpha}(\mathcal{E}) \\ \hat{\beta}(\mathcal{E}) \\ \hat{\gamma}(\mathcal{E}) \end{bmatrix} = \frac{1}{\sqrt{\alpha^2(\mathcal{E}) + \beta^2(\mathcal{E}) + \gamma^2(\mathcal{E})}} \begin{bmatrix} \alpha(\mathcal{E}) \\ \beta(\mathcal{E}) \\ \gamma(\mathcal{E}) \end{bmatrix}, \tag{31}$$

where $C_0 = 1$ is a constant that balances the x weights. The minimum and maximum of v_x, δ, and $G_q(n_0)$ can be determined according to the environmental conditions. The exponent σ is selected to balance the weight of the three metrics. The weights can penalize the metrics in the final cost function with the adjustment of σ. For instance, to achieve this goal, the change trend of $\alpha(\mathcal{E})$ w.r.t. $\tilde{v}_x^{\sigma_\alpha(v_x)}$ similar to that of $\sigma_\alpha(v_x)$ w.r.t. v_x. Other exponents have the same feature.

3) The weighted summation of the evaluation metrics is calculated by

$$S(\mathcal{E}, \Delta\boldsymbol{\theta}) = \hat{\alpha}(\mathcal{E})\kappa(\Delta\boldsymbol{\theta}) + \hat{\beta}(\mathcal{E})\phi_m(\Delta\boldsymbol{\theta}) + \hat{\gamma}(\mathcal{E})a_w(\Delta\boldsymbol{\theta}), \tag{32}$$

which is the final cost function. Then on each Pareto front, select the decision tuple with the minimal cost function value $S(\mathcal{E}, \Delta\boldsymbol{\theta})$ as the optimal structural parameters under the corresponding environmental condition, i.e., the "trade-off point".

Seeking the trade-off point differs from the conventional weighted-sum optimization method, which converts an MOO problem into a single-objective optimization problem [38]. The summation process here is performed on the Pareto fronts. Hence, the optimality of the solution can be guaranteed. After performing the trade-off point seeking procedure, the optimal change amounts of the adjustable parameters can be determined. The pipeline procedure of the proposed method is illustrated in Fig. 4.

5. Simulation results

5.1. Selection of parameters

Numerical experiments were performed under the driving scenarios de- scribed in Section 3 to demonstrate the effectiveness of the proposed method. The predetermined base $\boldsymbol{\theta}_0$ and the bounds of $\Delta\boldsymbol{\theta}$ are presented in Table 1(a), according to the common structure of sedan cars. The other parameters adopted in the modeling process are shown in Table 1b. In Table 1a, $(.)_0$ denotes the basic value of the parameter

Table 1
Adjustable and main fixed parameters of the active transformable vehicle.

(a)

Parameters	$(\cdot)0$	$\Delta(\cdot)$	$\Delta(\cdot)$
a/m	1.4	−0.2	0.2
L/m	2.7	−0.3	0.1
k_s/N·m^{-1}	22,500	−2500	2500
C_s/N·(m·s^{-1})$^{-1}$	1300	−100	500
h/m	0.8	−0.15	0.25
B/m	1.6	−0.1	0.2

(b)

Parameters	Symbol	Value
Total mass/kg	m	1420
Initial yaw moment inertia/(kg·m^2)	I_z0	1311
Initial roll moment inertia/(kg·m^2)	I_x	582
Linear stiffness of tires/(N·m^{-1})	k_t	225,000
Initial height of front roll center/m	h_f0	0.3
Initial height of rear roll center/m	h_r0	0.5
Position of vertical vibration test point/m	l	0.75
Ratio between sprung and unsprung mass	μ_{ss}	0.9

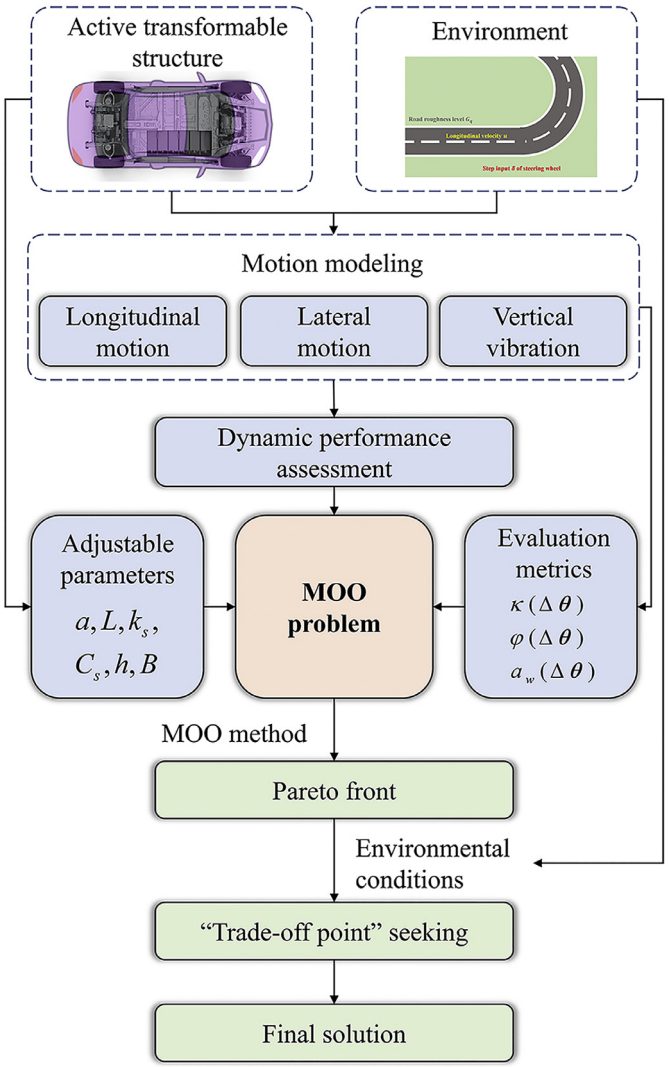

Fig. 4. Schematic of multi-objective optimization pipeline aided by active structural transformation.

and $\Delta()$, $\underline{\Delta()}$ denote the lower and upper bounds of the change amount, respectively.

5.2. Examples of Pareto fronts

By optimizing the evaluation metrics with NSGA-II, a series of Pareto fronts can be generated. Fig. 5 illustrates examples of Pareto fronts under different environmental conditions, which are set to (a) v_x=18 km/h, $G_q(n_0)=2^{10}\times0.6\times10^{-6}$ m^3, δ=0.1 rad in Fig. 5a, (b) v_x=36 km/h, $G_q(n_0)=2^{10}\times0.8\times10^{-6}$ m^3, δ=0.15 rad in Fig. 5b and (c) v_x=54 km/h, $G_q(n_0)=2^{10}\times1.0\times10^{-6}$ m^3, δ=0.2 rad in Fig. 5c. The adjustable and fixed parameters of the test car are presented in Table 1(a) and (b), respectively. The population size and maximum generation of NSGA-II were both set to 100. The results reveal a trade-off between different optimization objectives when the environmental conditions are fixed. For instance, by adopting the structural parameters in Zone 1 of the optimization objective space, the car might have less κ and ϕ_m but a greater a_w, leading to better handling stability but inferior ride comfort. When adopting the structural parameters in Zone 2, the car might have less ϕ_m and a_w but a greater κ. The ride experience might be improved, but the precision of the transient response is sacrificed. Moreover, when the environmental condition changes, the Pareto front moves in the space generated by the optimization objectives. In such cases, the method of making the "final decision" or a "trade-off point" according to the customized user requirements is essential.

After conducting the trade-off point seeking procedure, the set of optimal change amount of adjustable parameters $\Delta\theta_m(E)$ can be determined. Specifically, we chose $\sigma_\beta(\delta)=\sigma_\gamma(v_x)=\sigma_\gamma(G_q(n_0))=1$ and $\sigma_\alpha(v_x)=\sigma_\beta(v_x)=2$ as the exponents in (31) according to the sensitive analysis of the evaluation metrics w.r.t. the environmental parameters $\mathcal{E}$. Fig. 6 illustrates the decreasing amount of the three evaluation metrics of the car applying the proposed optimization scheme compared to a fixed-structure vehicle, with the environment parameters v_x, δ and $G_q(n_0)$ varying in a wide but feasible range for the J-turn. All evaluation metrics decrease to different degrees under different values of v_x, δ and $G_q(n_0)$. The reduction in κ and ϕ_m can reach up to 50–60 % in some scenarios, significantly improving the vehicle safety. The decrease in κ implies the reduction of the side-slip possibility at sharp corners. Limiting ϕ_m can reduce the risk of rollover and even approach the goal of "no rollover" if other structural parameters are well designed. This may help avoid more than half the traffic accidents involving vehicle handling [39]. Meanwhile, a decrease in a_w can provide passengers with a more comfortable ride experience. Furthermore, because of the trade-off point seeking method, the effectiveness of optimization can also be guaranteed in a scenario with high longitudinal speed and high road roughness. This helps improve safety and ride comfort under extreme conditions. Notably, the decreasing amount of the evaluation metrics compared with the conventional car varies in different scenarios. This also relates to the trade-off point seeking method, which dynamically adjusts the weight of different metrics according to the variation of driving conditions. From the simulation results it can be concluded that the proposed dynamic performance optimization method aligns with the goal of SDV technologies: achieving higher flexibility and freedom to offer a better user experience.

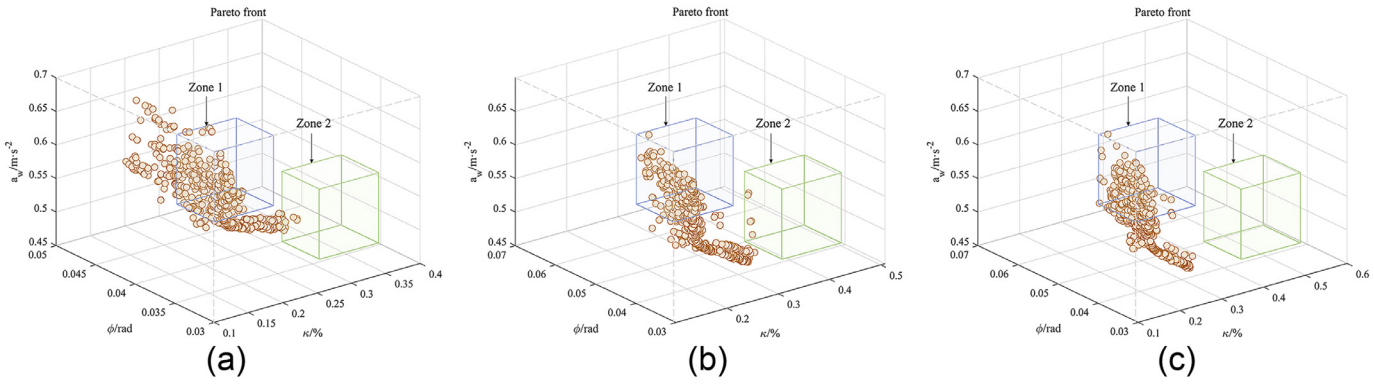

Fig. 5. Pareto fronts in different environmental conditions derived by the NSGA-II method.

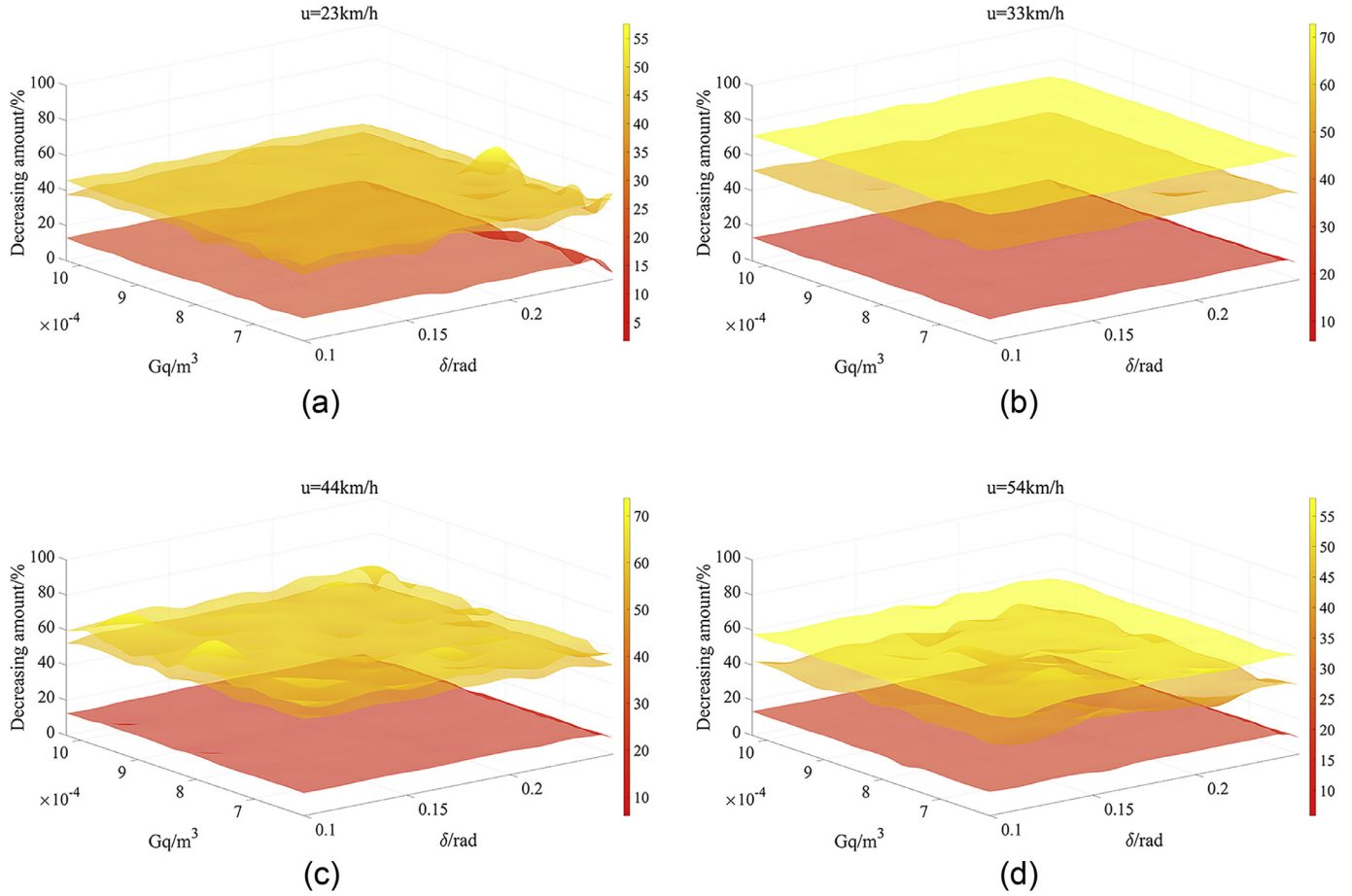

Fig. 6. Decreasing amounts of the evaluation metrics in different environmental conditions (comparing active transformable vehicles with conventional vehicles).

Fig. 7. Driving scenarios for validation.

Table 2
Environmental conditions of Scenarios A, B and C.

Test scenarios	Scenario A	Scenario B-I	Scenario B-II	Scenario C
v_x/(km/h)	18	36	36	54
δ/rad	0.1	0.15	0.15	0.2
$G_q(n_0)$/m^3	$2^{10} \times 0.81$ $\times 10^{-6}$	$2^{10} \times 0.62$ $\times 10^{-6}$	$2^{10} \times 0.81$ $\times 10^{-6}$	$2^{10} \times 0.62$ $\times 10^{-6}$

5.3. Simulations in certain driving scenarios

To prove the effectiveness of the proposed method more intuitively, three real test scenarios are selected for experimental validation. They are the square in front of the Main Building at Tsinghua University, the parking lot in front of the Art Museum at Tsinghua University when empty, and the open space at the northwest gate of Shougang Park in Shijingshan District, Beijing, China, designated as scenarios A, B and C, respectively (Fig. 7). By applying their environmental parameters, simulation-based verification is performed. The test sections are of the type demonstrated in Fig. 1. Scenario B comprises two road segments with different roughness levels. The environmental conditions are presented in Table 2, among which the power spectral density of the road roughness is estimated from the type of road surface. It is assumed that the driver drives a conventional car and then an active structural transformable car on the test road. The test car is first on the straight road with constant longitudinal speed v_x. After entering the curved road, the driver gives a certain steering angle and keeps it constant until the end of the test. The road excitation is assumed to be ideal white noise with finite bandwidth. To provide sufficient data support for the ride comfort evaluation, the test in each scenario is repeated several times to accumulate 1000s of simulation results. When the environmental conditions change, the structural parameters of the active transformable vehicle are assumed to change linearly over time.

The performances of the conventional and active transformable vehicle are compared, as shown in Fig. 8. The symbol "CV-A/SDV-A" implies the results of the conventional / active transformable vehicle in Scenario A. The ordinate in (c) measures the ratio of the current vertical vibration amplitude to the maximum amplitude of the conventional vehicle. Statistical evaluation metrics of the ratio, including the average energy on the time domain **E** and the standard deviation STD, are given in Table 3. The value before "/" is obtained from the conventional car, while that after "/" is obtained from the active transformable SDV. The total normal force T on the inside wheels is also compared according to Eq. 10, in order to assess the possibility of rollover. The assessment begins at 0.5 s after the step input of the steering angle to avoid the influence of

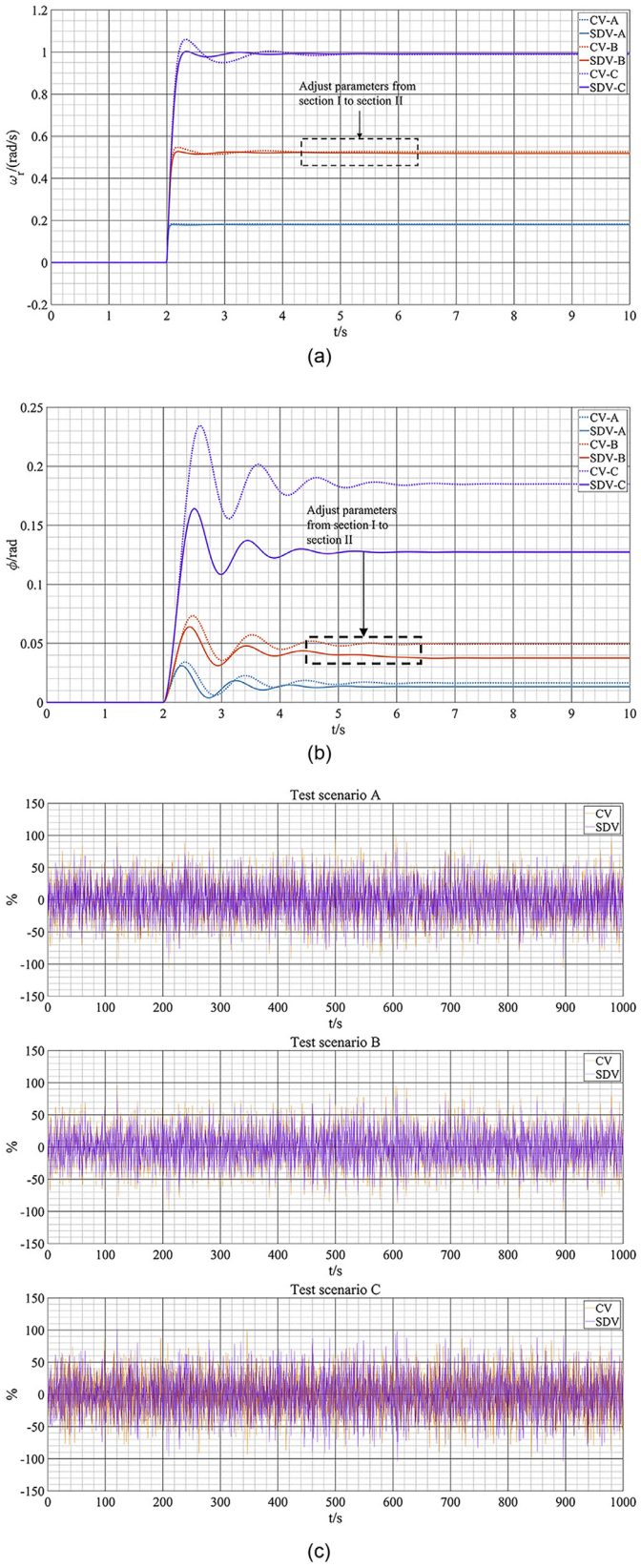

Fig. 8. Comparison of handling stability and riding performances of conventional and active transformable vehicles.

Table 3
Statistical metrics of amplitude ratio in vertical vibration evaluation.

Metrics	Scenario A	Scenario B	Scenario C
E	0.0699/0.0645	0.0606/0.0646	0.0612/0.0680
STD	0.2644/0.2539	0.2541/0.2462	0.2608/0.2474

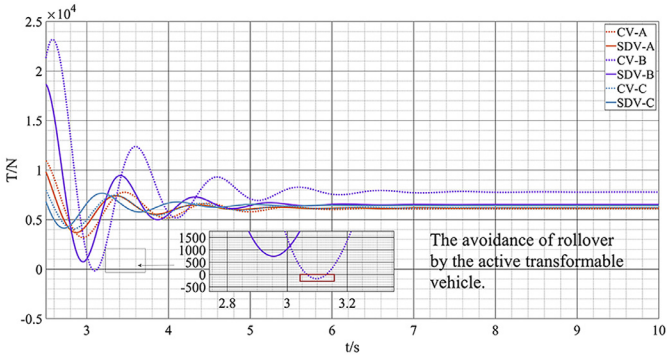

Fig. 9. Total normal forces on inside wheels for rollover possibility assessment.

a sudden change of $\ddot{\phi}$ in the simulations. The results are illustrated in Fig. 9.

The simulation results revealed that the test active transformable vehicle had a considerable advantage over the conventional vehicle in dynamic performance in all test scenarios. When the step input of the steering angle was given at a certain longitudinal speed, the overshoot of the yaw rate ω_r, the peak of the roll angle ϕ and the fluctuation amplitudes of the vertical displacement z_{sf} (t) and $z_{sr}(t)$ were effectively limited by adjusting the structural parameters online. The effect of the optimization was pronounced at high longitudinal speeds. The evaluation metrics κ and ϕ_m were quite high in high-speed cornering. If the former was too high, the accuracy of the transient response was reduced. If the latter was too high, rollover accidents were more likely to occur. The comparison in Fig. 9 illustrates that through online adjustment of structural parameters, the probability of rollover accidents was reduced especially in the high-speed cornering scenario, because the value of T of the active transformable vehicle was generally greater than that of the conventional vehicle and remained positive in all test cases. Regarding ride comfort, the vertical vibration acceleration level a_w decreased by over 15 % in all test scenarios. This indicates that the proposed method overcame the contradiction between handling and ride comfort in the usual sense, and realizes the simultaneous optimization of multiple dynamic performances.

For a vehicle with fully-functional software-defined technology, the selection of structural parameters is not only influenced by the dynamic performance requirements. User needs also play an important role. The boundaries of the adjustable parameters were set to simulate the influence of user needs. In fact, the selected metrics varied monotonically with respect to some structural parameters, such as h and B. Lower h and higher B always lead to better dynamic performance. The changes of these two parameters in the simulation also verify this statement. However, in practice, these parameters are bounded by other factors, such as user preferences. In the context of the “software-defined” concept, users are provided with more freedom to customize their vehicles. The flexible physical structure provides various choices, which is nearly impossible for conventional vehicles.

6. Conclusion

The trend toward SDVs will be irreversible. In this context, it is considerably important to investigate the potential advantages of SDV technologies further and present concretely and mathematically the concepts derived from them. Similar to the changes in the EE, software

architecture, and vehicular networks, the innovation in physical structure and hardware configuration is also an essential characteristic of the concept of SDVs. In contrast to conventional vehicles, active structural transformation technology makes the hardware configuration of the vehicle more extensible to support rich customized services better and improve the user experience.

Considering the ongoing research on the physical transformation of vehicles, this study explored the optimization of vehicle dynamic performance for a safer and more comfort driving experience in different driving scenarios utilizing active structural transformation technology. A mathematical model of the active transformable vehicle regarding motion dynamics was constructed. To achieve real-time performance enhancement, an MOO problem was proposed, considering key structural parameters as design variables and evaluation metrics of dynamic performance as optimization objectives. The simulation results revealed that, compared with a conventional fixed-structure vehicle, the active transformable vehicle applying the proposed method can adaptively obtain a better dynamic performance under different environmental conditions. The possibility of serious accidents, such as rollover, can be reduced under extreme conditions. Consequently, driving safety and ride comfort can be improved. Taking the enhancement of dynamic performance as an example, the study demonstrates the impact of the innovation in hardware architecture on future vehicles. This can provide insight for further research of future SDV.

Declaration of competing interest

The authors declare that they have no conflicts of interest in this work.

Acknowledgments

This research is sponsored in part by the NSFC Program (61872217, U20A20285, 52122217, 52221005, U1801263), in part by the National Key R&D Program of China (2020YFB1710901, 2018YFB1308601), and in part by the Jiangxi Provincial Natural Science Foundation under Grant 20224ACB218002.

References

[1] O. Burkacky, J. Deichmann, G. Doll, et al., in: Rethinking Car Software and Electronics Architecture, McKinsey & Co, 2018, p. 11.
[2] J. Ohlsen, The software-defined vehicle is overwhelming the automotive industry, ATZ Electron. Worldw. 17 (6) (2022) 56.
[3] R.N. Charette, This car runs on code, IEEE Spectr. 46 (3) (2009) 3.
[4] A. Klavmark, T. Vikingsson, Study on Open Source In-vehicle Infotainment (ivi) Software Platforms, Chalmers University of Technology, University of Gothenburg, 2015.
[5] S. Fürst, J. Mössinger, S. Bunzel, et al., Autosar–a world-wide standard is on the road, in: 14th International VDI Congress Electronic Systems for Vehicles, Baden-Baden, Vol. 62, 2009, pp 5.
[6] H. Bo, D. Hui, W. Dafang, et al., Basic concepts on autosar development, in: 2010 International Conference on Intelligent Computation Technology and Automation, 1, IEEE, 2010, pp. 871–873.
[7] S. Fürst, M. Bechter, Autosar for connected and autonomous vehicles: the autosar adaptive platform, in: 2016 46th annual IEEE/IFIP International Conference on Dependable Systems and Networks Workshop (DSN-W), IEEE, 2016, pp. 215–217.
[8] G.A. Lodi, A. Ott, S.A. Cheema, et al., Power line communication in automotive harness on the example of local interconnect network, in: 2016 International Symposium on Power Line Communications and its Applications (ISPLC), IEEE, 2016, pp. 212–217.
[9] Y. Tang, D. Zhang, D.W. Ho, et al., Tracking control of a class of cyber-physical systems via a flexray communication network, IEEE Trans. Cybern. 49 (4) (2018) 1186–1199.
[10] T. Chowdhury, E. Lesiuta, K. Rikley, et al., Safe and secure automotive over- the-air updates, in: International Conference on Computer Safety, Re-liability, and Security, Springer, 2018, pp. 172–187.
[11] S. Halder, A. Ghosal, M. Conti, Secure over-the-air software updates in connected vehicles: a survey, Comput. Netw. 178 (2020) 107343.
[12] M. Adnan, J. Iqbal, A. Waheed, et al., On the design of efficient hierarchic architecture for software defined vehicular networks, Sensors 21 (4) (2021) 1400.
[13] M.M. Islam, M.T.R. Khan, M.M. Saad, et al., Software-defined vehicular network (sdvn): a survey on architecture and routing, J. Syst. Archit. 114 (2021) 101961.
[14] T. Mekki, I. Jabri, A. Rachedi, et al., Software-defined networking in vehicular networks: a survey, Trans. Emerg. Telecommun. Technol. 33 (10) (2022) e4265.
[15] X. Liao, Z. Wang, X. Zhao, et al., Cooperative ramp merging design and field implementation: a digital twin approach based on vehicle-to-cloud communication, IEEE Trans. Intell. Transp. Syst. 23 (5) (2021) 4490–4500.
[16] M.S. Salek, S.M. Khan, M. Rahman, et al., A review on cybersecurity of cloud computing for supporting connected vehicle applications, IEEE Internet Things J. 9 (11) (2022) 8250–8268.
[17] B. Yang, R. Baines, D. Shah, et al., Reprogrammable soft actuation and shape-shifting via tensile jamming, Sci. Adv. 7 (40) (2021) eabh2073.
[18] V. Consumi, J. Merlin, L. Lindenroth, et al., A novel soft shape-shifting robot with track-based locomotion for in-pipe inspection, arXiv preprint arXiv:2202.10840 (2022).
[19] M. Gerbl, J. Gerstmayr, Self-reconfiguration of shape-shifting modular robots with triangular structure, Robot. Auton. Syst. 147 (2022) 103930.
[20] R.B. Scharff, G. Fang, Y. Tian, et al., Sensing and reconstruction of 3-d deformation on pneumatic soft robots, IEEE/ASME Trans. Mechatron. 26 (4) (2021) 1877–1885.
[21] W.-H. Wang, X.-J. Xu, H.-J. Xu, et al., Enhancing lateral dynamic performance of all-terrain vehicles using variable-wheelbase chassis, Adv. Mech. Eng. 12 (5) (2020) 1687814020917776.
[22] A. Soltani, A. Goodarzi, M.H. Shojaiefard, et al., Developing an active variable-wheelbase system for enhancing the vehicle dynamics, Proc. Inst. Mech. Eng. Part D: J. Auto. Eng. 231 (12) (2017) 1640–1659.
[23] Y. Jiang, X. Xu, L. Zhang, Heading tracking of 6wid/4wis unmanned ground vehicles with variable wheelbase based on model free adaptive control, Mech. Syst. Signal Process. 159 (2021) 107715.
[24] A. Soliman, M. Kaldas, Semi-active suspension systems from research to mass-market–a review, J. Low Freq. Noise Vib. Act. Control 40 (2) (2021) 1005–1023.
[25] D.-S. Yoon, G.-W. Kim, S.-B. Choi, Response time of magnetorheological dampers to current inputs in a semi-active suspension system: modeling, control and sensitivity analysis, Mech. Syst. Signal Process. 146 (2021) 106999.
[26] X. Jin, J. Wang, S. Sun, et al., Design of constrained robust controller for active suspension of in-wheel-drive electric vehicles, Mathematics 9 (3) (2021) 249.
[27] T. Gordon, L. Palkovics, C. Pilbeam, et al., Second generation ap- proaches to active and semi-active suspension control system design, in: The Dynamics of Vehicles on Roads and on Tracks, CRC Press, 2021, pp. 158–171.
[28] M. Lee, K. Lee, K. Hwang, et al., Development of a foldable micro electric vehicle for future urban driving with intelligent control, in: 17th International IEEE Conference on Intelligent Transportation Systems (ITSC), IEEE, 2014, pp. 2486–2491.
[29] I.-S. Suh, K. Hwang, M. Lee, et al., In-wheel motor application in a 4wd electric vehicle with foldable body concept, in: 2013 International Electric Machines & Drives Conference, IEEE, 2013, pp. 1235–1240.
[30] H.B. Pacejka, E. Bakker, The magic formula tyre model, Veh. Syst. Dyn. 21 (S1) (1992) 1–18.
[31] H. Pacejka, Tire and Vehicle Dynamics, Elsevier, 2005.
[32] R.N. Jazar, Vehicle Dynamics, 1, Springer, 2008.
[33] H. Yin, Y.-H. Chen, D. Yu, Rendering optimal design in controlling fuzzy dynamical systems: a cooperative game approach, IEEE Trans. Ind. Inform. 15 (8) (2018) 4430–4441.
[34] R. Yu, Y.-H. Chen, B. Han, Cooperative game approach to robust control design for fuzzy dynamical systems, IEEE Trans. Cybern. 52 (7) (2020) 7151–7163.
[35] D. Whitley, A genetic algorithm tutorial, Stat. Comput. 4 (2) (1994) 65–85.
[36] S. Mirjalili, Genetic algorithm, in: Evolutionary Algorithms and Neural Networks, Springer, 2019, pp. 43–55.
[37] K. Deb, A. Pratap, S. Agarwal, et al., A fast and elitist multiobjective genetic algorithm: nsga-ii, IEEE Trans. Evol. Comput. 6 (2) (2002) 182–197.
[38] N. Gunantara, A review of multi-objective optimization: methods and its applications, Cogent Eng. 5 (1) (2018) 1502242.
[39] V. Trucks, European Accident Research and Safety Report 2mi3, Volvo Trucks, Technical Report, Gothenburg, Sweden, 2013.

Bowei Zhang received the B.E. degree from the School of Vehicle and Mobility, Tsinghua University, Beijing, China, in 2021, where he is currently working toward the Ph.D. degree. His research interests include dynamics and control of autonomous vehicles and software-defined vehicle technologies.

Jin Huang received the B.E. and Ph.D. degrees from the College of Mechanical and Vehicle Engineering, Hunan University, Changsha, China, in 2006 and 2012, respectively. He is also a joint Ph.D. Student with the George W. Woodruff School of Mechanical Engineering, Georgia Institute of Technology, Atlanta, GA, USA, from 2009 to 2011. Then, he started his career as a Postdoctoral Fellow and an Assistant Research Professor at Tsinghua University, Beijing, China, in 2013 and 2016, respectively. His research interests include artificial intelligence in intelligent transportation systems, dynamics control, and software-defined vehicle technologies.